

# Analyzing and Synthesizing Images by Evolving Curves with the Osher-Sethian Method

RON KIMMEL

*Mail-Stop 50A-2152, Lawrence Berkeley Laboratory, University of California, Berkeley, CA 94720*

ron@math.lbl.gov

NAHUM KIRYATI

*TECHNION, Electrical Engineering Department, Haifa 32000, Israel*

nk@tx.technion.ac.il

ALFRED M. BRUCKSTEIN

*TECHNION, Computer Science Department, Haifa 32000, Israel*

freddy@cs.technion.ac.il

*Received October 3, 1995; Accepted March 28, 1996*

**Abstract.** Numerical analysis of conservation laws plays an important role in the implementation of curve evolution equations. This paper reviews the relevant concepts in numerical analysis and the relation between curve evolution, Hamilton-Jacobi partial differential equations, and differential conservation laws. This close relation enables us to introduce finite difference approximations, based on the theory of conservation laws, into curve evolution. It is shown how curve evolution serves as a powerful tool for image analysis, and how these mathematical relations enable us to construct efficient and accurate numerical schemes. Some examples demonstrate the importance of the CFL condition as a necessary condition for the stability of the numerical schemes.

**Keywords:** shape from shading, halftoning, offsets, distance maps, minimal geodesics, segmentation, numerical methods

## 1. Introduction

Recently, researchers in the field of image processing and computer vision started to pay attention to new ways of analyzing and representing two-dimensional, stationary or moving images, via planar curve evolution. In fact, any image can be viewed as a set of level curves “evolving” with the height parameter. Even such a simple description is quite useful in a variety of situations.

Several image analysis algorithms nowadays are based on propagating planar curves in the image plane according to local variations in the grey-level of the image (Bruckstein, 1994; Kimmel, 1995). Those planar contours might be, for example, the level sets on the

surface of an object whose shaded image we are trying to interpret so as to recover its three-dimensional structure. The Shape-from-Shading field is indeed a good example illustrating the way curve propagation algorithms found a very interesting application (Bruckstein, 1988). Their usefulness in this and other applications was further enhanced by the recent development, in the field of numerical analysis, of a “miraculous” algorithm for the stable propagation of planar curves according to a variety of rules (Osher and Sethian, 1988). This algorithm together with some recent results in the theory of curve evolution also resulted in powerful tools for edge preserving image smoothing (Alvarez et al., 1992, 1993; Weickert, 1995).

Other fields in which there were immediate consequences of having a stable and efficient way to propagate curves, are Computer Aided Design, Robotics, Shape Analysis and Computer Graphics.

In CAD there is a need to find offset curves and surfaces, implying fixed-speed curve propagation. Geodesic deformable models were introduced for shape modeling and analysis. In Computer Graphics, Pnueli and Bruckstein found an interesting application in the design of a clever half-toning method they named **Dig<sub>D</sub>ürer**.

In Robotics, where one often needs to find a path for robots that need to move from a source to a certain destination, one could determine shortest routes by propagating a wave of possibilities, and finding out the way its wavefront reaches the destination point. This is like Feynman's particles sniffing all possible paths before deciding on the trajectory of minimal action (Feynman et al., 1964) This, by the way, can be done even in the presence of moving obstacles. Last, but not least, we shall mention the field of Mathematical Morphology, where there is a need to precisely compute various types of distance functions, to enable erosion or dilation of shapes.

The solution for some of the problems that we will describe is based on the ability to find a new curve-evolution-based formulation to the problem. This new formulation is of the form of a differential equation that describes the propagation of a planar curve in time, under the constraints imposed by the problem. While propagating a planar curve one must often overcome various problems such as topological changes, e.g., a single curve that splits into two separate curves, and numerical problems that may be caused by the type of curve representation used, e.g., the problem of determining the offset curve to a polynomial parametric curve.

The most general propagation rule for a closed planar curve in time along its normal direction  $\vec{N}$  is

$$\frac{\partial \mathcal{C}}{\partial t} = V \vec{N} \quad \text{given } \mathcal{C}(0),$$

where  $\mathcal{C}(s, t) : S^1 \times [0, T] \rightarrow \mathbb{R}^2$  is the curve description and  $V$  is a smooth scalar velocity function. The function  $V$  may depend on local properties of the curve or on some external control variable like for example the image gray level or terrain traversability<sup>1</sup>. Let  $\phi(x, y, t)$  be an implicit representation of the curve so that  $\mathcal{C}(s, t) = \{(x, y) \mid \phi(x, y, t) = 0\}$ , i.e., the zero level set of a time varying surface function  $\phi(x, y, t)$ . Then, the propagation rule for  $\phi$  that yields the correct curve propagation equation is given by (Osher and

Sethian, 1988).

$$\frac{\partial \phi}{\partial t} = V |\nabla \phi| \quad \text{given } \phi^{-1}(0) = \mathcal{C}(0).$$

In some of the problems it is natural to use a given image  $I$  as initialization for the implicit function  $\phi(x, y, 0) = I$ .

The implicit representation of the propagating curve solves numerical and topological problems of the propagation. Tracking the *zero level set* of the bivariate function  $\phi(x, y)$  propagating in time, overcomes these problems in an elegant way, and leads to the desired numerical scheme. This new formulation for the implementation of propagating curves is due to Osher and Sethian (1988), who called it the *Eulerian* formulation.

In Section 2 some classical problems are presented, and the curve evolution solutions to these problems are shortly described. Sections 3 through 9 present guide lines for constructing numerical schemes for the curve evolution equations. The importance of the CFL condition is illustrated by several examples in Section 10.

## 2. Variations on a Theme

### 2.1. Shape from Shading

A classical problem in the area of computer vision is how to reconstruct a 3D surface  $z(x, y)$  from a given gray-level picture  $I(x, y)$ . In (Bruckstein, 1988; Kimmel, 1992; Kimmel et al., 1995b), it is shown that under reasonable assumptions about the light source and the object reflection properties, it is possible to solve this problem by using the image data to control the evolution of a planar curve so as to track the equal height contours of the object. Those equal height contours refer to equal heights with respect to the light source direction (Kimmel and Bruckstein, 1995b). Some analytic manipulations on the relations between the contours and the data leads to an evolution rule for a planar curve. This evolution rule, in which the propagation time indicates the height with respect to the light source direction  $\hat{l} = (-p_l, -q_l, 1)/\sqrt{1 + p_l^2 + q_l^2}$ , is determined by the gray-level image and the local nature of the curve. For the simplest shading rule  $I = \langle \hat{l}, \hat{n} \rangle$ , see Fig. 1, the planar evolution of the equal height (with respect to  $\hat{l}$ ) is given by

$$c_t = \frac{F(x, y) \sqrt{n_1^2(1 + q_l^2) + n_2^2(1 + p_l^2) - n_1 n_2 2 p_l q_l - (p_l n_1 + q_l n_2)}}{\sqrt{1 + p_l^2 + q_l^2}} \cdot \vec{N},$$

where  $\vec{N} = (n_1, n_2)$  is the normal to the curve and  $F(x, y) = I(x, y)/\sqrt{1 - I(x, y)^2}$ ,  $I(x, y)$  being the

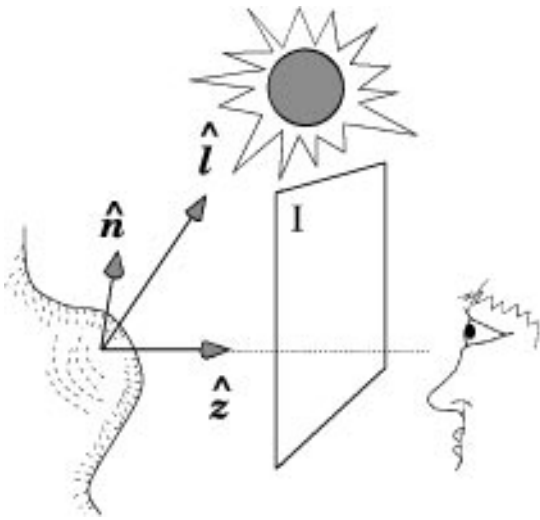


Figure 1. According to the simplest shading rule  $I = (\hat{l}, \hat{n})$ , where  $\hat{n}$  is the surface normal.

shaded image. The implicit, Eulerian, formulation in this case is:

$$\phi_t = \frac{F(x,y)\sqrt{\phi_x^2(1+q_t^2) + \phi_y^2(1+p_t^2) - \phi_x\phi_y 2p_tq_t - (p_t\phi_x + q_t\phi_y)}}{\sqrt{1+p_t^2+q_t^2}}$$

In (Kimmel and Bruckstein, 1995a) we have shown how to use “weighted distance transforms” implied by the shape from shading curve evolution for each of the singular points in the shading image to solve the global shape from shading problem for smooth surfaces (Morse functions). See Fig. 2 (taken from (Kimmel and Bruckstein, 1995a)).

### 2.2. Gridless Halftoning—The Dig<sup>i</sup>ürer

Using the image data to control the evolution of a planar curve can also be used to generate graphical

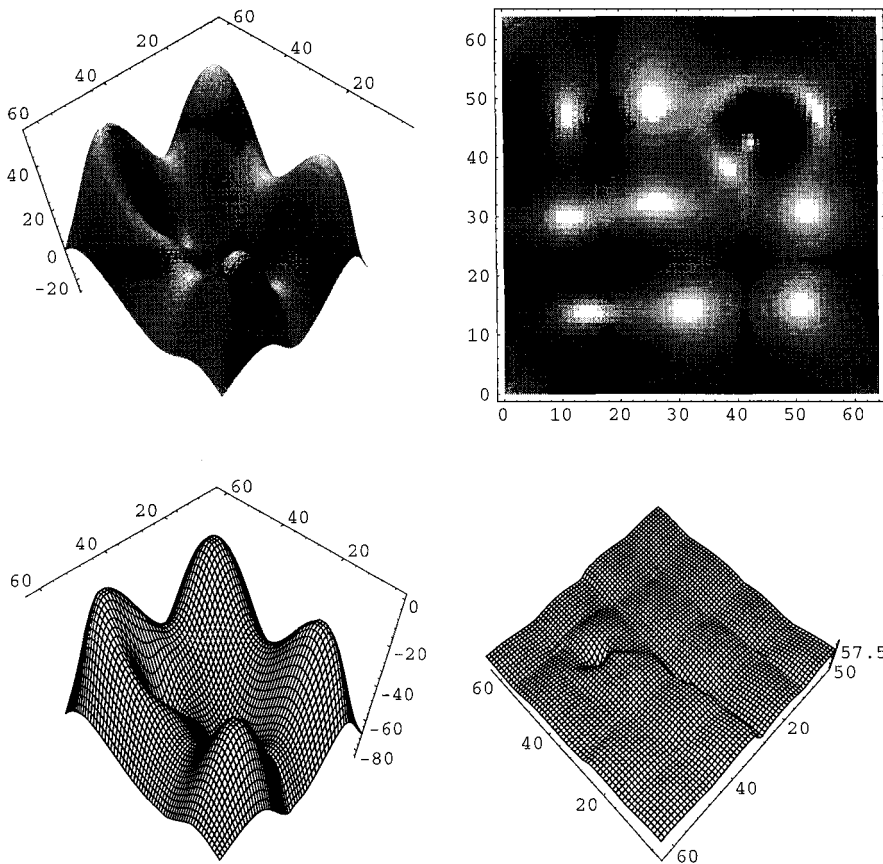


Figure 2. A smooth synthetic surface on the upper left produces the shading image on the upper right frame. The reconstruction of the 3D shape from the shading image, based on Morse smoothness assumption is displayed on the lower left, and the error of subtracting the reconstruction from the original surface on the lower right.

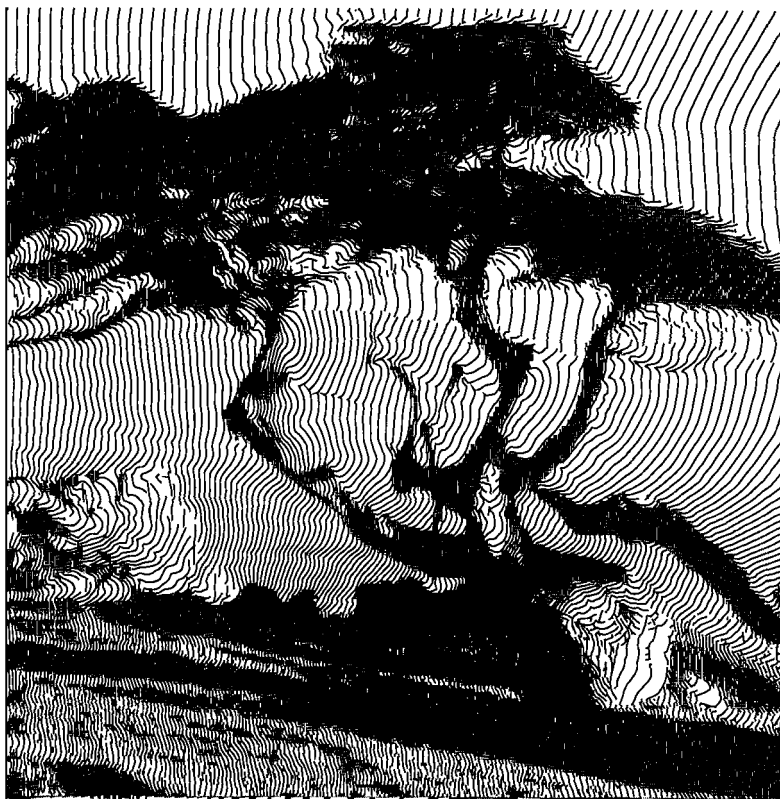


Figure 3. Propagating a planar curve with a velocity proportional to the image gray levels results in an artistic approach for half-toning.

effects. One such application for gray and color half-toning is the **Dig<sub>D</sub>ürer**, that aims to emulate the work of classical engravers (Pnueli and Bruckstein, 1994, 1996; Schroeder, 1983). Figure 3, taken from (Pnueli and Bruckstein, 1994), shows the result of propagating a planar curve controlled by the image intensity.

A rough description of this evolution is

$$C_t = F(I(x, y))\vec{N},$$

where  $F: \mathbb{R}^+ \rightarrow \mathbb{R}^+$  is a monotone function. The implicit formulation is:

$$\phi_t = F(I(x, y))|\nabla\phi|.$$

### 2.3. Continuous Scale Morphology

In the field of shape theory, it is often required to analyze a shape by activating some “morphological” operations that make use of a “structuring element” with some given shape, see Fig. 5. In (Sapiro et al., 1993), the problem of morphological operators in which the element may be of any convex shape with variable sizes

was explored (Brockett and Maragos, 1992), see also (Alvarez et al., 1993). This problem too may be reformulated as the problem of activating a propagation rule for the shape’s boundary. The evolution rule for the shape’s boundary is determined by the structuring element’s shape  $r(\theta)$ , and the time of evolution in this case represents the size of the element. The planar evolution of the boundary curve is

$$C_t = \sup_{\theta} (r(\theta), \vec{N})\vec{N},$$

see Fig. 4, and the Eulerian evolution is given by

$$\phi_t = \sup_{\theta} (r(\theta), \nabla\phi).$$

### 2.4. Shape Offsets or Prairie Fire Propagation

In CAD (computer aided design) one often encounters the need to find the offset of a given curve. A simple algorithm that solves this problem may be constructed by considering a curve that propagates with a constant velocity along its normal direction at each point (Kimmel and Bruckstein, 1993; Blum, 1973). The propagation time represents the “offset distance”

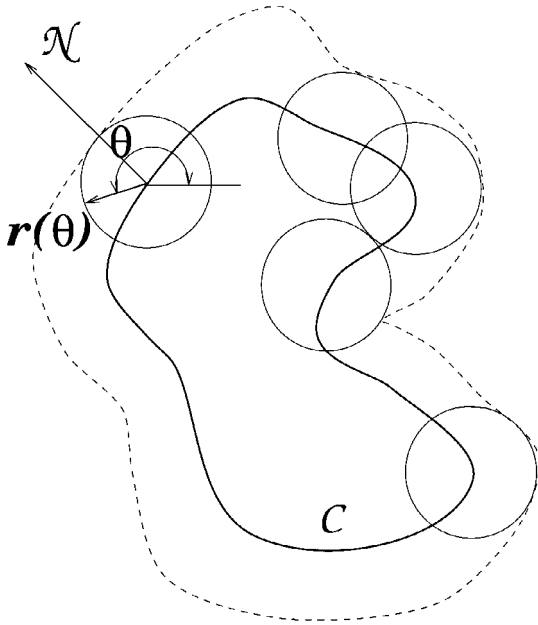


Figure 4. Dilation operation with a circle structuring element. In this case, since  $\sup_{\theta} (r(\theta), \vec{N}) = 1$  the evolution rule is simply  $C_t = \vec{N}$  (i.e., the offsetting/prairie-fire problem).

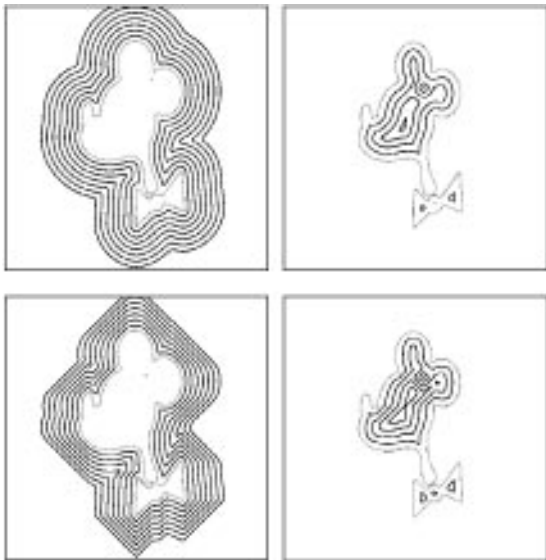


Figure 5. A dilation and erosion operations with diamond and circle structuring elements of different scales.

from the given curve, and the evolution rule is simply

$$C_t = \vec{N},$$

its implicit Eulerian formulation being

$$\phi_t = |\nabla\phi|.$$

This is, of course, also Blum's prairie fire propagation model for finding shape skeleton, i.e., the shock fronts of the propagation rule.

## 2.5. Minimal Geodesics on Surfaces

This important problem in the field of robotic navigation may be solved by considering an equal distance contour propagating from a point on a given surface. In (Kimmel et al., 1995c), an analytic model that describes the propagating 3D curve, was introduced. Tracking such a 3D curve is quite a complicated task. However, it is also possible to follow its projection on the plane, see Fig. 6.

Calculating the 3D distance maps by tracking the projected evolution from both source and destination points on the given surface, enables us to select the shortest path which is given by the minimal level set in the sum of the two distance maps, see Fig. 7. The propagation time in this case, indicates distance on the surface, i.e., the geodesic distance. The planar evolution is

$$C_t = \sqrt{\frac{(1+q^2)n_1^2 + (1+p^2)n_2^2 - (2pq)n_1n_2}{1+p^2+q^2}} \vec{N},$$

where  $p = dz/dx$  and  $q = dz/dy$  are the gradient components of the surface  $z(x, y)$ , and  $\vec{N} \equiv (n_1, n_2)$  is the planar normal. The Eulerian (implicit) evolution in this case is

$$\phi_t = \sqrt{\frac{(1+q^2)\phi_x^2 + (1+p^2)\phi_y^2 - (2pq)\phi_x\phi_y}{1+p^2+q^2}}.$$

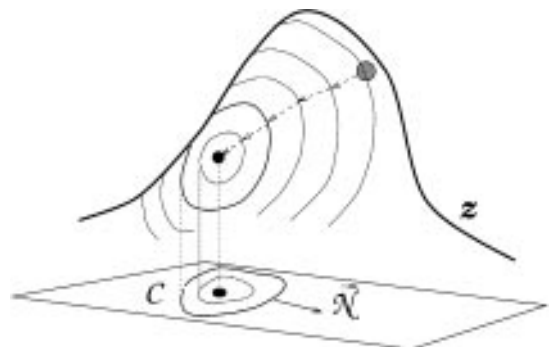


Figure 6. Projecting the equal geodesic distance contour evolution to the coordinate plane, simplifies the geodesic distance computation.

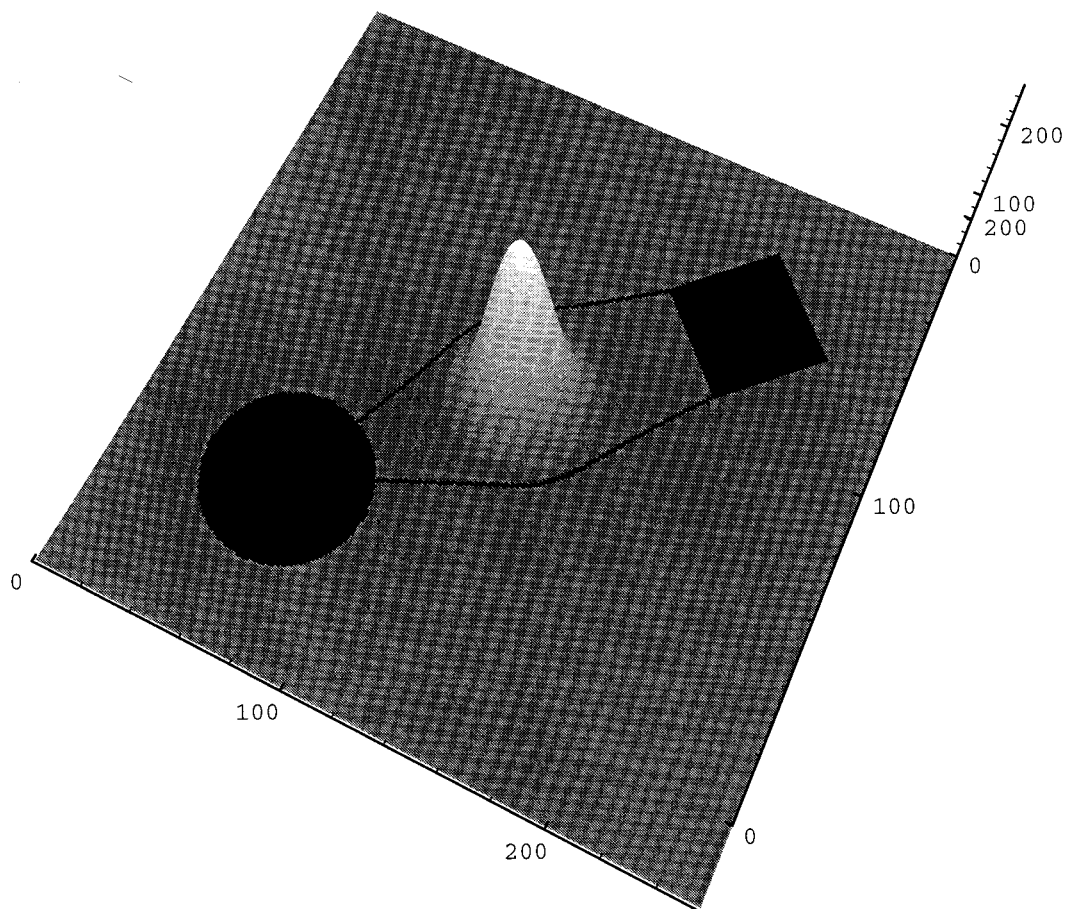


Figure 7. Finding the paths of minimal length between the square and circle areas on a Gaussian mountain surface.

### 2.6. Shortening Three Dimensional Curves via Two Dimensional Flows

Given a path connecting two points on a given surface, it is sometimes required to shorten its length locally and to find the closest geodesic to the given curve. In (Kimmel and Sapiro, 1995) it is shown that this operation too may be done by propagating a curve along the geodesic curvature. This 3D curve propagation may also be performed by tracking its planar projection, and may be used to refine minimal geodesics obtained by other methods, e.g., the minimal path estimation obtained by the Kiryati-Székely algorithm (1993).

### 2.7. Distance Maps and Weighted Distance Transforms

As stated in (Kimmel et al., 1996d), some of the above results may in fact be grouped under the same title of

‘generalized distance maps’. While searching for off-set curves, one constructs the distance transform. Reconstructing the shape from shading may be shown to be equivalent to calculating a weighted distance transform. Continuous scale morphology, may be shown to result in the distance transform under a given metric, where the structuring element of the morphological operations defines the unit sphere of the given metric.

### 2.8. Using Multi-Valued Distance Maps in Path Planning on Surfaces with Moving Obstacles

In (Kimmel et al., 1995) the *multi valued* distance map concept is introduced. A multi valued distance map is defined and used as a tool for computing optimal path for a robot with limited velocity navigating on a surface and avoiding moving obstacles. The distance map on the given surface incorporates the constraints imposed by the moving obstacles and is produced by curve propagation techniques. The basic idea of our

method is the use of Huygens principle leading to a wave front propagating in time and describing the farthest parts the robot could arrive to by moving in all possible ways away from the source region. Clearly, the minimal path to the destination will be determined when this wave front first meets the destination. In some sense, the method proposed searches over all possible spatio-temporal robot movements to determine the time-optimal navigation path and schedule to the required destination. Although it may seem obvious that this process will discover the best navigation course, it is far from trivial to realize how one could actually carry out this program in a computationally efficient way. The limit on the robot velocity is used to reduce the complexity of the problem from a search over a 3D configuration space to a search over a 2D multi valued array. The analytic analysis as well as efficient numerical algorithms for calculating the multi valued distance map and tracking an optimal path are introduced.

### 2.9. Skeletons via Level Sets

“Skeletons are thin, exact descriptors of shapes”, (Shaked and Bruckstein, 1996). Defining the distance of a point from a curve as the infimum of distances between the point to the set of curve points. The skeleton of a shape is the set of internal points whose distance to the boundary is realized in more than one boundary point. Each point of the skeleton is associated with a width descriptor corresponding to its distance from the boundary.

Being a stick figure, or naive description of the shape, skeletons are perceptually appealing. From a pattern recognition point of view, skeletons provide a unique combination of boundary and area information. Although mathematically well defined (in the continuous plane), it has always been a problem to implement skeletons on computers. This situation has brought numerous suggestions of solutions referred to as skeletonization or thinning algorithms.

Having a stable scheme describing distances in the digital plane, solves many of the inherent problems of skeletonization. As shown in (Kimmel et al., 1995a), skeletons are located on zero crossing curves of differences of distance transforms from boundary segments. Applying simple differential geometry results to skeletons, it is possible to find a necessary and sufficient partition of the boundary to segments whose distance transforms participate in the specification of the skeleton location. See Fig. 8 (taken from (Kimmel et al., 1995a)).

### 2.10. Geometric Invariant Flows

The relation between the Eulerian formulation and curve evolution serves as a direct link between curve and image evolution. Under some limitations, like preserving the order of level sets (preserving the embedding), it is possible to evolve all the level sets simultaneously. Each of the evolving level sets will follow the same evolution rule. This important observation made it possible to extend the Euclidean scale space of planar curves (Grayson, 1987; Gage and Hamilton, 1986) into geometric image smoothing, and the affine scale space of curves into affine invariant image smoothing (Sapiro and Tannenbaum, 1993; Alvarez et al., 1992; Alvarez et al., 1993).

The Euclidean *geometric heat equation* is given by

$$C_t = \kappa \vec{\mathcal{N}},$$

where  $\kappa$  is the curvature. The Eulerian formulation is

$$\phi_t = \nabla \cdot \left( \frac{\nabla \phi}{|\nabla \phi|} \right) |\nabla \phi|.$$

The affine *geometric heat equation* may be geometrically written as

$$C_t = \kappa^{1/3} \vec{\mathcal{N}},$$

with Eulerian formulation

$$\phi_t = \nabla \cdot \left[ \left( \frac{\nabla \phi}{|\nabla \phi|} \right) \right]^{1/3} |\nabla \phi|,$$

that simplifies into

$$\phi_t = (\phi_{xx}\phi_y^2 - 2\phi_x\phi_y\phi_{xy} + \phi_{yy}\phi_x^2)^{1/3}.$$

### 2.11. Geodesic Active Contours

One of the main problems in image analysis is the segmentation problem. Given several objects in an image it is necessary to integrate their boundaries in order to achieve good model of the objects under inspection. This problem was addressed in many ways over the years, starting with simple thresholding, region growing, and deformable contours based on energy minimization along a given contour called ‘snakes’.

In (Caselles et al., 1995a; 1995b) a novel geometric model that starts from a user defined contour and segments objects in various type of images is introduced. The idea is to minimize a total ‘non-edge’ penalty function  $g(x, y)$  integrated along the curve. The relation to the classical snakes and to recent geometric models is explored, showing better behavior of the proposed

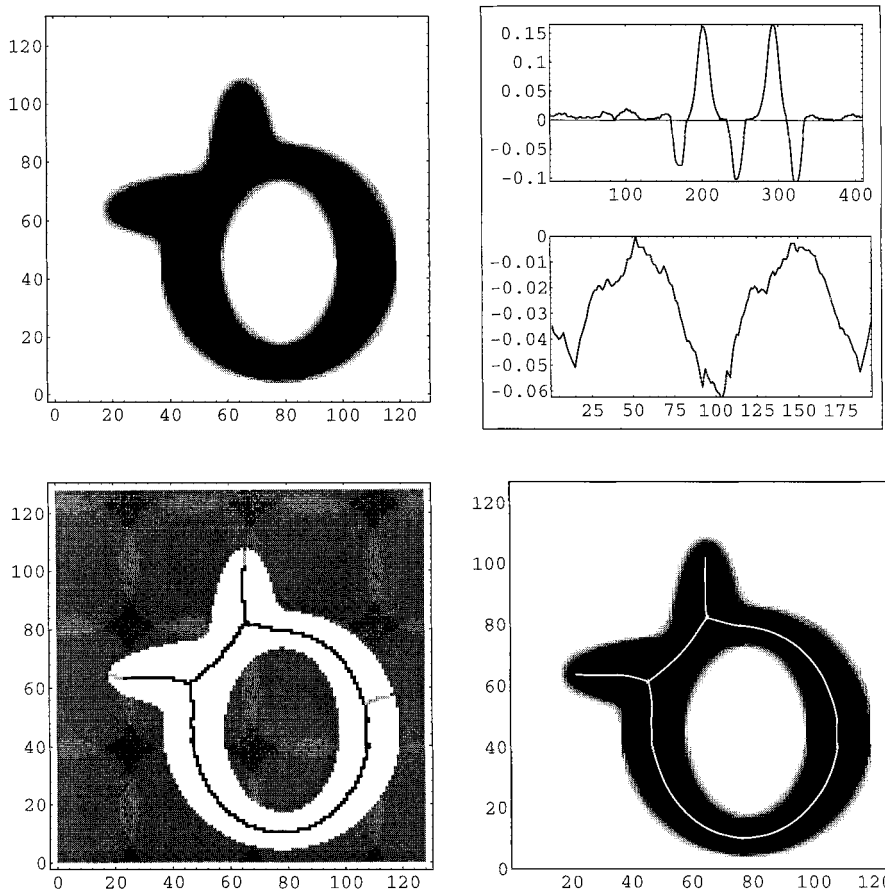


Figure 8. Finding the skeleton of the shape in the upper left frame is done by first locating the curvature positive maxima along the boundaries on the upper right. Then, by calculating the distance from each boundary segment, the skeleton may be determined with sub-pixel accuracy as shown in the lower right frame.

method over its ‘ancestors’: The classical snakes and the recent geometric models. The planar evolution of the boundary curve is

$$\mathcal{C}_t = ((c + \kappa)g - \langle \nabla g, \vec{N} \rangle) \vec{N},$$

where  $c$  is an arbitrary constant, and  $\kappa$  is the curvature. The Eulerian evolution in this case is given by

$$\phi_t = \left( c + \nabla \cdot \left( \frac{\nabla \phi}{|\nabla \phi|} \right) \right) g |\nabla \phi| - \langle \nabla g, \nabla \phi \rangle.$$

The tumor in the Fig. 9 (taken from (Caselles et al., 1997)) is an *acousticus neurinoma*, and includes the triangular shaped portion at the top left part. The detection process is presented on the zoom out part of the tumor on the right. For comparison, the same image was also applied to the model developed in (Caselles et al., 1993; Malladi et al., 1995). Due to the large variation of the gradient along the object boundaries and the high noise in the image, the curve did not stop at

the correct position, it shrinks to a point and the tumor was not detected.

This way of finding local geodesics in a potential function defined by an edge detection operator requires an initial contour as initial conditions. In some other cases, it is desired to locate the minimal geodesic connecting two points along the boundary of an object. In (Cohen and Kimmel, 1997) an approach of integrating edges by locating the minimal geodesic is explored. See Fig. 10 (taken from (Cohen and Kimmel, 1997)).

### 3. Numerical Schemes and the Eulerian Formulation

The procedures required for in solving some of the classical problems we deal with are in fact procedures for solving partial differential equations (PDEs). In the following sections we give a brief introduction

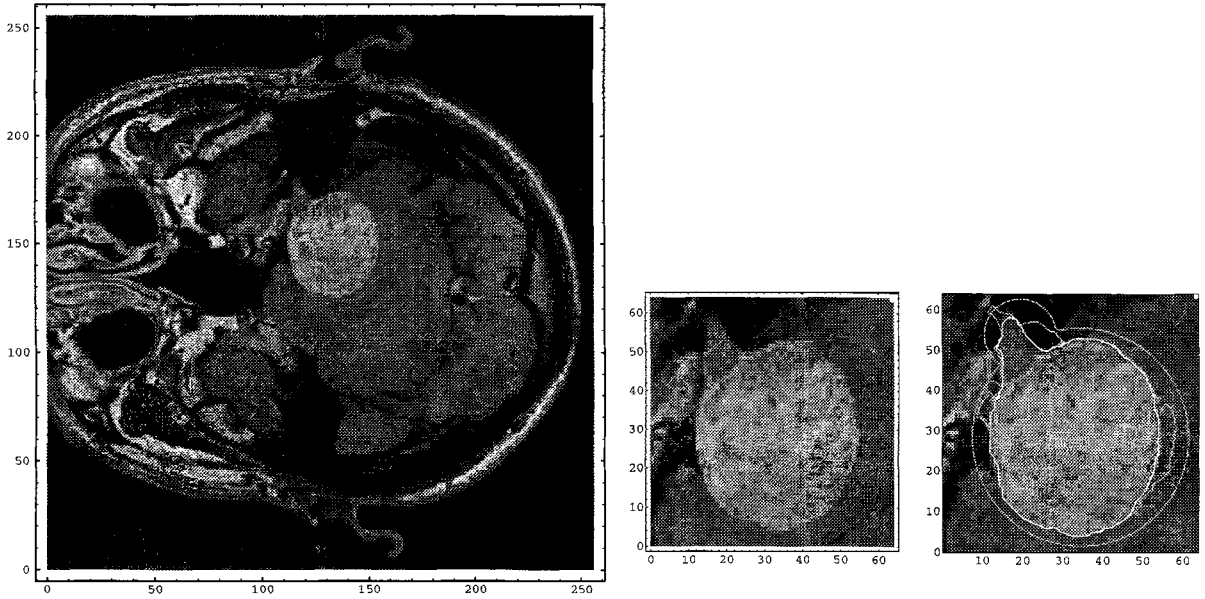


Figure 9. An example of tumor detection in MRI via geodesic active contours. The tumor in the image on the left is an *acousticus neurinoma*, and includes the triangular shaped portion at the top left part. For this image, an inward deforming contour was used. The tumor portion on the right is shown after zoom out for better presentation. The gray contours are the positions of the evolving curve in time, while the white contour is the final result of segmenting the tumor.

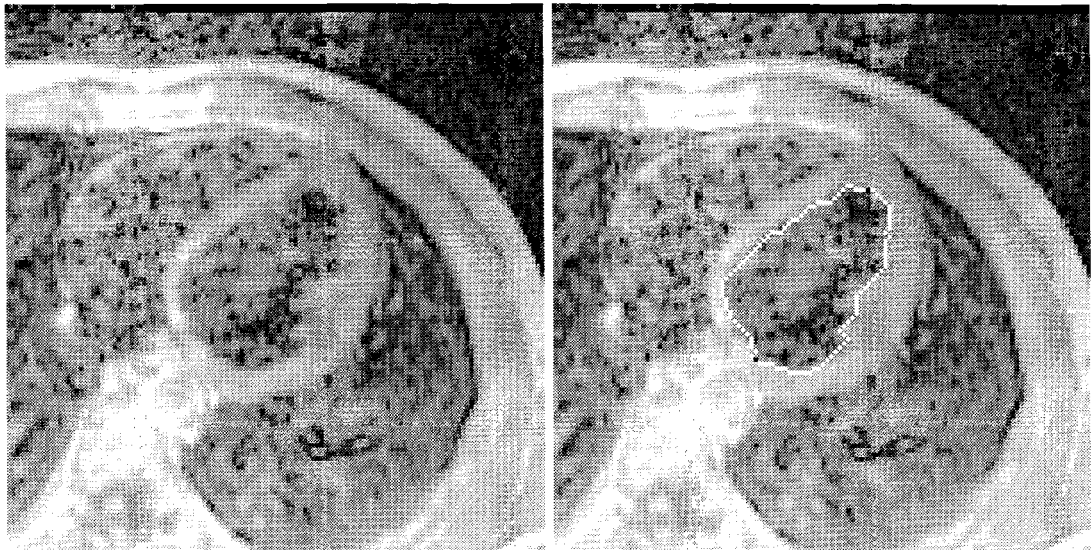


Figure 10. An MR heart image on the left. The white contour between the two black end points on the right is the segmentation result of the desired ventricle.

to numerical analysis issues that were found relevant for approximation, when solving such PDE's. We present the basics of how to select the proper numerical scheme for approximating a given evolution equation. Planar curve evolutions are reformulated as Hamilton-Jacobi (HJ) equations. Then, using the close relation between hyperbolic conservation laws and HJ

equations, numerical schemes that make use of this relation are discussed. The purpose of this paper is to stress the practical usage of the numerical methods, therefore basic concepts and recipes are presented in a simple and often simplistic way that we hope will be of help for potential future implementers of such methods.

#### 4. Helpful Literature

The numerical analysis literature that best fits our needs, deals with numerical approximations of Hamilton Jacobi equations. As shown in (Osher and Sethian, 1988) these equations are closely related in nature to hyperbolic conservation laws. Therefore, numerical techniques that were developed for approximating the evolution of differential conservation laws may readily be adapted to the type of equations we encounter.

The book of LeVeque (1992) is a great help as an introduction to numerical methods for conservation laws. The interested reader could find more detailed information of the basic concepts and definitions in this book. Formal definitions and limitations of numerical methodologies as applied to conservation laws in fluid dynamics may be found in (Sod, 1985). More information about conservation laws and the theory of shock waves, is given by one of the founders of this theory, Peter D. Lax, in his lecture notes (Lax, 1973). The theory of shock waves and its applications in the analysis of gas dynamics is given by Smoller in the third part of his book (Smoller, 1983).

The relation between conservation laws and the evolution of curves was introduced by Osher and Sethian in their classic paper (Osher and Sethian, 1988). In this paper, Osher and Sethian present a new formulation for curve evolution by considering the evolution of a higher dimensional function in which the curve is embedded as a level set. The relation of this evolution process to conservation laws is explored, stable and efficient numerical schemes being proposed. Other, more general, (e.g., for non convex Hamiltonians) numerical schemes approximating the same type of PDE's may be found in (Osher and Shu, 1991).

The search for better numerical schemes in this field is still an ongoing concern of many researchers. Although several new techniques have been introduced since the book of LeVeque was published, we still feel that "the mathematical theory is lagging behind the state-of-the-art computational methods" (LeVeque, 1992).

#### 5. Basic Definitions

The continuous case analysis is of course very important when analyzing PDE's. However (although accurate analysis serves an important role in understanding the behavior of the equation) when implementing a numerical approximation of such an equation

on a digital computer one must address several other topics as well.

An example of a very simple, yet very important, question is how to approximate  $u_x(x)$ , the first derivative of the function  $u(x) : \mathbb{R} \rightarrow \mathbb{R}$  in the  $x$  direction. Let us simplify the problem and assume that  $u(x)$  is sampled by taking uniform samples of its values at equal distances of  $\Delta x$ . Denote  $u_i$  to be its  $i$ -th sample, i.e.,  $u_i \equiv u(i\Delta x)$ , and  $D^x u_i$  as the *finite difference approximation* of the function  $u$  at the point  $x = i\Delta x$ . In approximating  $u_x$  one should consider computation efficiency, accuracy and consistency with the continuous case. Using the samples it is possible to interpolate a smooth function passing through the function values at the sample points. A very simple approximation is the *centered* difference finite approximation, given by

$$D^x u_i \equiv \frac{u_{i+1} - u_{i-1}}{2\Delta x}.$$

It is based on the Taylor series expansion, with a truncation error of  $\mathcal{O}(\Delta x^2)$ .

The *forward* finite approximation is similarly defined as

$$D_+^x u_i \equiv \frac{u_{i+1} - u_i}{\Delta x},$$

and the *backwards* approximation:

$$D_-^x u_i \equiv \frac{u_i - u_{i-1}}{\Delta x}.$$

In both cases above, the truncation error is of  $\mathcal{O}(\Delta x)$ .

Taking  $\Delta x \rightarrow 0$  the approximation obviously converges to the continuous case for the case of smooth functions. Convergence to the continuous case is an important issue that is referred to as *consistency* with the continuous case.

#### 6. Conservation Laws and Hamilton-Jacobi Equations

The curve evolution equations are differential rules describing the change of the curve, or its evolution, in 'time'. As we shall see in the next section there is a formulation that puts curve evolution equations into a closely related formulation having the flavor of conservation laws. Following (Lax, 1973): A conservation law asserts that the rate of change of the *total amount* of substance contained in a fixed domain  $G$  is equal to the *flux* of that substance across the boundary of  $G$ . Denoting the *density* of that substance by  $u$ , and

the flux by  $f$ , the conservation law is

$$\frac{d}{dt} \int_G u dx = - \int_{\partial G} \langle f, n \rangle dS,$$

where  $n$  denotes the outwards normal to  $G$  and  $dS$  the surface element on  $\partial G$ , which is the boundary of  $G$ , so that the integral on the right measures the outflow—hence the minus sign. Applying the divergence theorem, taking  $d/dt$  under the integral sign, dividing by the volume of  $G$  and shrinking  $G$  to a point where all partial derivatives of  $u$  and  $f$  are continuous we obtain the *differential conservation law*:

$$u_t + \nabla \cdot f = 0.$$

Consider the simple 1D case in which the integral (by  $x$  and  $t$ ) version of a conservation law gets the explicit form of:

$$\int_{x_0}^{x_1} (u(x, t_1) - u(x, t_0)) dx + \int_{t_0}^{t_1} (f(x_1, t) - f(x_0, t)) dt = 0.$$

A solution  $u$  is called a *generalized solution* of the conservation law if it satisfies the above integral form for every interval  $(x_0, x_1)$  and every time interval  $(t_0, t_1)$ . Taking  $x_1 \rightarrow x_0$ ,  $t_1 \rightarrow t_0$ , and dividing by the volume  $dxdt = (x_1 - x_0)(t_1 - t_0)$ , we obtain the 1D differential conservation law:

$$u_t + f_x = 0.$$

For  $f_x = (H(u))_x$ , (i.e., assuming  $f$  is a function of  $u$  given by  $H(u)$ ) a *weak solution* of the above equation is defined as  $u(x, t)$  that satisfies (Sethian, 1989)

$$\frac{d}{dt} \int_{x_0}^{x_1} u(x, t) dx = H(u(x_0, t)) - H(u(x_1, t)).$$

Weak solutions are useful in handling non smooth data. Observe further that  $u$  need not be differentiable to satisfy the above form, and they are not unique. Thus, we are left with the problem of selecting a special ‘physically correct’ weak solution.

The Hamilton-Jacobi (HJ) equation in  $\mathbb{R}^d$  has the form

$$\phi_t + H(\phi_{x_1}, \dots, \phi_{x_d}) = 0, \quad \phi(x, 0) = \phi_0(x).$$

Such equations appear in many applications. As pointed out in (Osher and Sethian, 1988; Osher and Shu,

1991), there is a close relation between HJ equations and hyperbolic conservation laws that in  $\mathbb{R}^d$  take the form

$$u_t + \sum_{i=1}^d f_i(u)_{x_i} = 0, \quad u(x, 0) = u_0(x).$$

Actually, for the one-dimensional case ( $d = 1$ ), the HJ equation is equivalent to the conservation law for  $u = \phi_x$ . This equivalence disappears when considering more than one dimension:  $H(\cdot)$  is often a non linear function of its arguments  $\phi_{x_i}$  and obviously does not have to be separable, so that we can no longer use the integration relation between  $\phi$  and  $u$ . However, numerical methodologies that were successfully used for solving hyperbolic conservation laws are still useful for HJ equations.

## 7. Entropy Condition and Vanishing Viscosity

In general, the weak solution for a conservation law is not unique and an additional condition is needed to select the *physically correct* or *vanishing viscosity* solution. This additional condition is referred to as the *entropy condition*.

Consider the ‘viscous’ conservation law:

$$u_t + (H(u))_x = \epsilon u_{xx}.$$

The effect of the viscosity  $\epsilon u_{xx}$  is to smear (or diffuse) the discontinuities, thereby, ensuring a unique smooth solution. Introducing the viscosity term turns the equation from a hyperbolic into a parabolic type, for which there always exists a unique smooth solution for  $t > 0$ . The limit of this solution as  $\epsilon \rightarrow 0$  is known as the ‘vanishing viscosity’ solution. The entropy condition selects the weak solution of the conservation law

$$u_t + (H(u))_x = 0 \quad u(x, 0) = u_0(x),$$

that is the vanishing viscosity solution for  $u_0$ . Therefore, the vanishing viscosity solution is sometimes referred to as the entropy solution.

Satisfying the entropy condition guarantees meaningful and unique weak solutions. Moreover, there is a close duality between the entropy condition and the Eulerian formulation to curve evolution. Actually, the search for an entropy condition for the case of curve evolution (Sethian, 1985) eventually led Osher and Sethian to the Eulerian formulation (1988) that will be described in the following section.

## 8. The Eulerian Formulation

The Eulerian formulation for planar curve evolution was first proposed by Osher and Sethian in (1988). This formulation allows the developments of efficient and stable numerical schemes in which topological changes of the propagating curve are automatically handled.

Consider the family of planar curves given by  $\mathcal{C}(s, t) : [0, L(t)] \times [0, T) \rightarrow \mathbb{R}^2$ , where  $s$  is the arclength of the curve  $\mathcal{C}$  at time  $t$ . Let the curve evolution equation describing the differential change of the curve in time be given by

$$\mathcal{C}_t = \mathcal{V}, \quad \mathcal{C}(s, 0) = \mathcal{C}_0(s),$$

where  $\mathcal{V}(s, t) : [0, L] \times [0, T) \rightarrow \mathbb{R}^2$ , is some velocity vector field that changes smoothly along the curve. The same evolution may be equivalently written by considering the normal  $\vec{\mathcal{N}} = \mathcal{C}_{ss}/|\mathcal{C}_{ss}|$  and tangential  $\vec{\mathcal{T}} = \mathcal{C}_s$  components of the velocity  $\mathcal{V}$  along the curve:

$$\mathcal{C}_t = \langle \mathcal{V}, \vec{\mathcal{N}} \rangle \vec{\mathcal{N}} + \langle \mathcal{V}, \vec{\mathcal{T}} \rangle \vec{\mathcal{T}}, \quad \mathcal{C}(s, 0) = \mathcal{C}_0(s).$$

A basic result from the theory of curve evolution is that the geometric shape of the curve (often referred to as the trace or the image of the planar curve) is only affected by the normal component of the velocity. The tangential component affects only the parameterization, and not the geometric shape of the propagating curve:

**Lemma 1 (Epstein and Gage, 1987).** *The family of curves  $\mathcal{C}(p, t)$  that solve the evolution rule*

$$\mathcal{C}_t = V_N \vec{\mathcal{N}} + V_T \vec{\mathcal{T}},$$

where  $V_N$  does not depend on the parameterization of the curve,<sup>2</sup> can be converted into the solution of

$$\mathcal{C}_t = V_N \vec{\mathcal{N}}.$$

**Proof:** Given  $\mathcal{C}(p, t) : S^1 \times [0, T) \rightarrow \mathbb{R}^2$  as the original family of curves, let  $p = p(\omega, \tau)$  and  $t = \tau$  with  $\partial p / \partial \omega > 0$  be a reparameterization. By the chain rule

$$\begin{aligned} \mathcal{C}_\tau &= \mathcal{C}_\omega \omega_\tau + \mathcal{C}_t t_\tau \\ &= \mathcal{C}_\omega \omega_\tau + \mathcal{C}_t. \end{aligned}$$

For the arclength parameterization  $s$  we have that

$$\begin{aligned} \mathcal{C}_\omega &= \mathcal{C}_s s_\omega \\ &= \vec{\mathcal{T}} s_\omega. \end{aligned}$$

Using these two expressions we calculate

$$\begin{aligned} \mathcal{C}_\tau &= \mathcal{C}_\omega \omega_\tau + \mathcal{C}_t \\ &= \vec{\mathcal{T}} s_\omega \omega_\tau + V_T \vec{\mathcal{T}} + V_N \vec{\mathcal{N}} \\ &= (V_T + s_\omega \omega_\tau) \vec{\mathcal{T}} + V_N \vec{\mathcal{N}}, \end{aligned}$$

Choosing the parameter  $\omega$  that solves the O.D.E.:

$$V_T + s_\omega \omega_\tau = 0,$$

and recalling the selection  $t = \tau$  we arrive at:

$$\mathcal{C}_t = V_N \vec{\mathcal{N}}. \quad \square$$

Therefore, since our interest is the shape of the curve we can consider the ‘Lagrangian’ form of the curve evolution:

$$\mathcal{C}_t = \langle \mathcal{V}, \vec{\mathcal{N}} \rangle \vec{\mathcal{N}}, \quad \mathcal{C}(s, 0) = \mathcal{C}_0(s),$$

and for  $V_N = \langle \mathcal{V}, \vec{\mathcal{N}} \rangle$ ,

$$\mathcal{C}_t = V_N \vec{\mathcal{N}}, \quad \mathcal{C}(s, 0) = \mathcal{C}_0(s). \quad (1)$$

While implementing the evolution given by the Lagrangian formulation one should handle topological changes in the evolving curve by external procedures. Such a procedure should monitor the process and detect possible mergings and splittings of the curve. It was also shown (Sethian, 1985; Osher and Sethian, 1988; Sethian, 1989) that such implementations are very sensitive to the formation of high curvature and sharp corners. The problems appear due to a time varying coordinate system  $(s, t)$  of the direct curve representation (where  $s$  is the parameterization, and  $t$ —the time). An initial smooth curve can develop curvature singularities. The question is how to continue the evolution after singularities appear. The natural way is to choose the solution which agrees with the *Huygens principle* (Sethian, 1985). Viewing the curve as the front of a burning flame, this solution states that *once a particle is burnt, it cannot be re-ignited* (Sethian, 1989). It can also be proved that from all the *weak* solutions of the Lagrangian formulation, the one derived from the Huygens principle is unique, and can be obtained by a constraint denoted as the ‘‘entropy condition for curve evolution (Osher and Sethian, 1988)’’.

In order to overcome these difficulties the ‘Eulerian formulation’ was proposed in (Osher and Sethian, 1988).

Let  $\phi(x, y, t) : \mathbb{R}^2 \times [0, T) \rightarrow \mathbb{R}$  be an implicit representation of the curve  $\mathcal{C}(s, t)$ , so that the zero level set  $\phi(x, y, t) = 0$  is the set of points constructing the curve  $\mathcal{C}(s, t)$ . In other words, the trace of the curve  $\mathcal{C}$

at time  $t$  is given by the zero level set of the function  $\phi$  at time  $t$ :

$$\mathcal{C}(t) = \phi^{-1}(0).$$

The demand of  $\mathcal{C}$  being the zero level set is arbitrary, and actually any other level set may serve the same purpose. The problem is how to evolve the  $\phi$  function in time so that its zero level set tracks the time varying curve  $\mathcal{C}(t)$ .

Denote by  $\nabla \equiv (\partial/\partial x, \partial/\partial y)$  the gradient operator. Then, from basic calculus, we have

**Lemma 2.** *The planar unit normal of the curve  $\mathcal{C} = \phi^{-1}(c)$ , where  $c$  is an arbitrary constant selecting the level set, is given by  $\vec{N} = \nabla\phi/|\nabla\phi|$ .*

**Proof:** Let  $s$  be the arclength parameter of  $\mathcal{C}$ . Then, along the equal height contour  $\mathcal{C}$  the change of  $\phi$  is zero:

$$\phi_s = 0 = \phi_x x_s + \phi_y y_s.$$

This expression  $\langle \nabla\phi, \mathcal{C}_s \rangle = 0$ , determines that  $\nabla\phi$  is orthogonal to  $\mathcal{C}_s = \vec{T}$ .  $\square$

According to the chain rule,

$$\phi_t = \phi_x x_t + \phi_y y_t.$$

Then, the above equation may be written as:

$$\begin{aligned} \phi_t &= \langle \nabla\phi, \mathcal{C}_t \rangle \\ &= \langle \nabla\phi, V_N \vec{N} \rangle \\ &= \left\langle \nabla\phi, V_N \frac{\nabla\phi}{|\nabla\phi|} \right\rangle \\ &= V_N \left\langle \nabla\phi, \frac{\nabla\phi}{|\nabla\phi|} \right\rangle \\ &= V_N |\nabla\phi|, \end{aligned}$$

which is the Eulerian formulation for curve evolution. Given **any** smooth function  $\phi_0(x, y)$  such that  $\phi_0^{-1}(0) = \mathcal{C}_0$  we can rewrite the last result

$$\phi_t = V_N |\nabla\phi|, \quad \phi(x, y, 0) = \phi_0(x, y), \quad (2)$$

which is a Hamilton-Jacobi type of equation. This formulation of planar curve evolution processes frees us from the need to take care of the possible topological changes in the propagating curve. Sethian (1989) named the above *Eulerian formulation* for front propagation, because it is written in terms of a fixed coordinate system.

The normal component  $V_N$  may be any smooth scalar function. An important observation is that any geometric property of the curve  $\mathcal{C}$  may be computed from its implicit representation  $\phi$ . The curvature, for example, plays an important role in many applications:

**Lemma 3.** *The curvature  $\kappa$  of the planar curve  $\mathcal{C} = \phi^{-1}(c)$  is given by*

$$\kappa = -\frac{\phi_{xx}\phi_y^2 - 2\phi_x\phi_y\phi_{xy} + \phi_{yy}\phi_x^2}{(\phi_x^2 + \phi_y^2)^{3/2}} \quad (3)$$

**Proof:** Along  $\mathcal{C}$ , the function  $\phi$  does not change its values. Therefore,  $\partial^n \phi / \partial s^n = 0$ , for any  $n$ . Particularly, for  $n = 2$ ,

$$\begin{aligned} 0 &= \frac{\partial^2 \phi}{\partial s^2} \\ &= \frac{\partial}{\partial s} (\phi_x x_s + \phi_y y_s) \\ &= \phi_{xx} x_s^2 + 2\phi_{xy} x_s y_s + \phi_{yy} y_s^2 + \phi_x x_{ss} + \phi_y y_{ss} \\ &= \phi_{xx} x_s^2 + 2\phi_{xy} x_s y_s + \phi_{yy} y_s^2 + \langle \nabla\phi, \mathcal{C}_{ss} \rangle. \end{aligned} \quad (4)$$

Recall that  $\vec{N} = (-y_s, x_s) = \nabla\phi/|\nabla\phi|$ , and that by definition  $\mathcal{C}_{ss} = (x_{ss}, y_{ss}) = \kappa \vec{N}$ . Or explicitly

$$\begin{cases} y_s = -\frac{\phi_x}{\sqrt{\phi_x^2 + \phi_y^2}} \\ x_s = \frac{\phi_y}{\sqrt{\phi_x^2 + \phi_y^2}}, \end{cases}$$

and

$$\begin{cases} x_{ss} = \kappa \frac{\phi_x}{\sqrt{\phi_x^2 + \phi_y^2}} \\ y_{ss} = \kappa \frac{\phi_y}{\sqrt{\phi_x^2 + \phi_y^2}}. \end{cases}$$

Introducing these two expressions into Eq. (4) we conclude that

$$\begin{aligned} 0 &= \frac{\phi_{xx}\phi_y^2 - 2\phi_x\phi_y\phi_{xy} + \phi_{yy}\phi_x^2}{|\nabla\phi|^2} + \langle \nabla\phi, \mathcal{C}_{ss} \rangle \\ &= \frac{\phi_{xx}\phi_y^2 - 2\phi_x\phi_y\phi_{xy} + \phi_{yy}\phi_x^2}{|\nabla\phi|^2} + |\nabla\phi|\kappa. \end{aligned}$$

$\square$

## 9. Numerical Methodologies

We have seen that the curve evolution may be presented as a Hamilton-Jacobi equation. In one dimension, the HJ equation coincides with hyperbolic conservation laws. This close relation can be used to construct numerical schemes for our problems. Similarly to the

continuous case, a finite difference method is in *conservation form* if it can be written in the form

$$\frac{u_j^{n+1} - u_j^n}{\Delta t} = - \frac{(g_{j+1/2}^n - g_{j-1/2}^n)}{\Delta x}, \quad (5)$$

where  $g_{j+1/2} = g(u_{j-p+1}, \dots, u_{j+q+1})$  is called a *numerical flux*, is Lipschitz<sup>3</sup> and *consistent* (satisfies the consistency requirement)

$$g(u, \dots, u) = H(u),$$

i.e., setting all the  $p+q$  variables of the numerical flux function to  $u$ , the numerical flux becomes identical to the continuous flux.

**Theorem 1.** *Suppose that the solution  $u(x, n\Delta t)$  of a finite difference method in conservation form converges to some function  $v(x, t)$  as  $\Delta x$  and  $\Delta t$  approach zero. Then  $v(x, t)$  is a weak solution of the continuous equation.*

The proof may be found in (Sod, 1985), p. 286.

A numerical scheme is *monotone* if the function  $F(u_{j-p}^n, \dots, u_{j+q+1}^n)$  that defines the scheme

$$u_j^{n+1} = F(u_{j-p}^n, \dots, u_{j+q+1}^n),$$

or equivalently (for a conservation form):

$$\begin{aligned} u_j^{n+1} &= F(u_{j-p}^n, \dots, u_{j+q+1}^n) \\ &= u_j^n - \frac{\Delta t}{\Delta x} (g_{j+1/2}^n - g_{j-1/2}^n), \end{aligned}$$

is a non-decreasing function of all its  $(p+q+1)$  arguments, that is,

$$F_j \equiv \frac{\partial F}{\partial u_{j+i}^n} \geq 0 \quad \text{for } -p \leq i \leq q+1.$$

**Theorem 2 (Kuznetsov, 1976)<sup>4</sup>.** *A consistent, monotone finite difference method  $u_j^n$  that has a conservation form, converges to the unique entropy satisfying weak solution of  $u_t - (H(u))_x = 0$ .*

The *local truncation error* measures how well the finite difference method models the differential equation locally. It is defined by replacing the approximated solution in the difference method by the true solution  $u(j\Delta x, n\Delta t)$ . Let us replace for example  $u_j^{n+1}$  by the Taylor series about  $u(x, t)$ , i.e.,  $u + \Delta t u_t + (1/2)\Delta t^2 u_{tt} + \dots$ . We do the same for the spatial derivatives, and arrive at the error bound that is a function of  $\Delta x$  and  $\Delta t$ . A first order accurate scheme is

a differential method with local truncation error (for  $\Delta t/\Delta x = \text{constant}$ ) of  $\mathcal{O}(\Delta t)$  (as  $\Delta t \rightarrow 0$ ).

Satisfying the entropy condition is indeed a desired quality however these schemes are limited by the following theorem:

**Theorem 3.** *A monotone finite difference method in conservation form is first order accurate.*

For proof see (Sod, 1985), p. 299.

Getting higher order accuracy for such equations by relaxing the monotonicity demand may be found in (Osher and Sethian, 1988; Osher and Shu, 1991). One idea leads to the essentially non-oscillating (ENO) schemes, in which an adaptive stencil is used between the discontinuities. Thereby, piecewise smooth data may be handled with high accuracy.

The relation between the Hamilton-Jacobi equations and the conservation laws may be used to design first order finite difference methods for the HJ equations (Osher and Sethian, 1988). The relation between  $\phi(x, t)$ , the solution of an HJ equation, and  $u(x, t)$ , the solution of the corresponding differential conservation law that describes the change of  $u = \text{'the slope of } \phi\text{'}$ , for the one dimensional case, is given by integration, i.e.,  $\phi(x, t) = \int_{-\infty}^x u(\tilde{x}, t) d\tilde{x}$ . Thus by integrating over the monotone numerical scheme (and shifting from  $j+1/2$  to  $j$ ) we arrive at

$$\Phi_j^{n+1} = \Phi_j^n - \Delta t g(D_- \Phi_{j-p+1}^n, \dots, D_+ \Phi_{j+q}^n).$$

**Definition 1.** An upwind finite difference scheme is defined so that

$$g_{j+1/2} = \begin{cases} H(u_j) & H' > 0 \\ H(u_{j+1}) & H' < 0 \end{cases}.$$

In some cases, an upwind numerical flux in a conservation form results in a monotone method<sup>5</sup>. The upwind monotone HJ scheme for the special case where

$$H(u) = h(u^2),$$

with  $h'(u) < 0$ , was introduced in (Osher and Sethian, 1988):

$$\begin{aligned} g_{\text{HJ}}(u_j^n, u_{j+1}^n) &= h((\min(u_j^n, 0))^2 \\ &\quad + (\max(u_{j+1}^n, 0))^2). \end{aligned}$$

This scheme has the advantage of being easy to generalize to more than one dimension.

Motivated by the theory of mathematical morphology (Brockett and Maragos, 1992), we have found the following scheme to have same qualities (being upwind) as the HJ scheme under the same restrictions

$(h'(u) < 0)$ :

$$g_M(u_j^n, u_{j+1}^n) = h((\max(-u_j^n, u_{j+1}^n, 0))^2).$$

This is Godunov's scheme for this case (see e.g., (Osher and Sethian, 1988)). The only difference between the  $g_{HJ}$  and the  $g_M$  is that at points where  $u$  changes from negative to positive magnitude,  $g_M$  selects the maximum between  $(u_j)^2$  and  $(u_{j+1})^2$ , while  $g_{HJ}$  selects  $(u_j)^2 + (u_{j+1})^2$ . We have found that the  $g_M$  numerical flux produces better results in some cases.

Having the numerical flux, or numerical Hamiltonian in the HJ context, we can write the numerical approximation of the Hamilton-Jacobi formulation as

$$\Phi_j^{n+1} = \Phi_j^n - \Delta t g(D_- \Phi_j^n, D_+ \Phi_j^n). \quad (6)$$

As we noted before, in some cases the requirements on the numerical scheme are relaxed to achieve higher order accuracy as well as handling more complicated flux functions. One useful example for our case is partial derivatives that are approximated by *slope limiters*. The idea is to keep the total variations of the evolving data under control, leading to the TVD (total variation diminishing) methods (LeVeque, 1992). By selecting the smallest slope between the forward and backward derivatives, the estimated slope of the data is always limited by the continuous data. A simple example of a first order slope limiter is given by the *minmod* operation. Define the *minmod* selection function as

$$\text{minmod}\{a, b\} = \begin{cases} \text{sign}(a)\min(|a|, |b|) & \text{if } ab > 0 \\ 0 & \text{otherwise} \end{cases}$$

This can be used to approximate  $\phi_x$  by the *minmod* finite derivative

$$\phi_x|_{x=i\Delta x} \approx \text{minmod}(D_+^x \Phi_i, D_-^x \Phi_i).$$

In (Osher and Sethian, 1988; Osher and Shu, 1991) it was shown that higher order accuracy can be easily achieved by using TVD methods for second order accuracy with solid theory, or using ENO method for higher order accuracy (in this case there is not yet a concrete theory for these working schemes). An important implementation issue introduced in (Adalsteinsson and Sethian, 1995), is the fact that performing computations only in a narrow band around the propagating front can reduce the computation effort. In this case, computations are performed in a narrow band that is dynamically swept with the front, while the rest of the grid points in the domain serve only as sign holders (see also (Chopp, 1993)).

## 10. The CFL Condition

One of the earliest observations in the field of finite difference schemes was made by Courant et al., (1928, 1967). They observed that a necessary stability condition for any numerical scheme is that the *domain of dependence* of each point in the domain of the numerical scheme should include the domain of dependence of the PDE itself. This condition is necessary, but not necessarily sufficient, for the stability of the scheme. For hyperbolic PDEs the domain of dependence is known to be bounded.

Considering the 1D case, when refining the discretization grid by letting  $\Delta x \rightarrow 0$  and  $\Delta t \rightarrow 0$ , the ratio  $\Delta t/\Delta x$  should be limited. This limit, known as the CFL number or the Courant number, is determined by the maximal possible flow of information. The flow lines of the information obviously depend on the specific initial data and are known as the *characteristics* of the PDE. Collisions of characteristics form 'shocks' in the solution and therefore require additional conditions which determine how to handle the propagation of such a shock. A propagating shock in time may thus be defined as a sequence of colliding characteristics where the entropy condition defines the speed of this propagation.

As a simple example consider the 1D conservation law in which the the point  $(x = \tilde{x}, t = \tilde{t})$  in the PDE domain can be influenced by the data bounded by the triangle  $(x_0, 0), (\tilde{x}, \tilde{t}), (x_1, 0)$ . This means that any information at the interval  $(x_0, x_1)$  of the initial condition  $u_0$  may influence the result at  $(\tilde{x}, \tilde{t})$ , namely  $u(\tilde{x}, \tilde{t})$ . Similarly, it may be asserted that the point  $(\tilde{x}, \tilde{t})$  is in the *domain of influence* of each point in the interval  $(x_0, x_1)$ . Therefore, any finite difference approximating the PDE should take this fact into consideration, by limiting the ratio  $\Delta t/\Delta x$ . Taking this to a limit, for  $u_t + (H(u))_x = 0$  the CFL restriction for a 3-point scheme can be shown to be

$$1 \geq \frac{\Delta t}{\Delta x} |H'|,$$

and in our case, where we have actually integrated a 3-point of  $\Delta x$  scheme of a conservation law into a 3-point HJ equation we arrive at the same CFL restriction.

As pointed out, the  $g_{HJ}$  and the  $g_M$  numerical flows may be easily generalized to several dimensions. The generalization is straightforward and for the specific case of  $H(u, v) = f(u^2, v^2)$  we get the following form

$$g_M(u_i^n, u_{i+1}^n, v_j^n, v_{j+1}^n) = h((\max(-u_i^n, u_{i+1}^n, 0))^2, (\max(-v_j^n, v_{j+1}^n, 0))^2)$$

This yields an upwind monotone scheme with a CFL restriction of

$$1 \geq \left( \frac{\Delta t}{\Delta x} |H_u| + \frac{\Delta t}{\Delta y} |H_v| \right).$$

Consider the simple example of a planar curve propagating with constant velocity along its normal that obeys the following evolution law,

$$C_t = \vec{N}.$$

It is easy to see that since  $V_N = 1$  the Eulerian formulation for this case is

$$\phi_t = |\nabla\phi|,$$

thus,  $H(u, v) = \sqrt{u^2 + v^2}$ . For the simple selection of  $\Delta x = \Delta y = 1$ , we arrive at the CFL restriction:

$$\Delta t \leq \frac{1}{\sqrt{2}}.$$

The following example presents offsets produced by two schemes, one with  $\Delta t < 1/\sqrt{2}$ , satisfying the CFL restriction, and another with  $\Delta t > 1/\sqrt{2}$ , violating the CFL restriction. The Eulerian formulation is implemented by the following numerical approximation:

$$\begin{aligned} \Phi_{ij}^{n+1} = & \Phi_{ij}^n + \Delta t \\ & \times \sqrt{\left( \max(-D_-^x \Phi_{ij}^n, D_+^x \Phi_{ij}^n, 0) \right)^2 + \left( \max(-D_-^y \Phi_{ij}^n, D_+^y \Phi_{ij}^n, 0) \right)^2}. \end{aligned}$$



Figure 11. The original image which is an implicit representation of the contours describing the outline of the letters in the image.

Figure 11 is the data image  $I$ , given as initial condition to the evolution equation ( $\Phi^0 = I$ ). The evolution of  $\Phi$  in time for the scheme with  $\Delta t = 0.7 < 1/\sqrt{2}$  is presented in Fig. 12. The offsetting results of the two schemes with  $\Delta t = 0.7$  and  $\Delta t = 0.8$  are presented in Fig. 13 on the left and right columns, respectively. The gray levels correspond to the height values of  $\Phi_{ij}^n$  on the grid. Histogram equalization is applied to the last

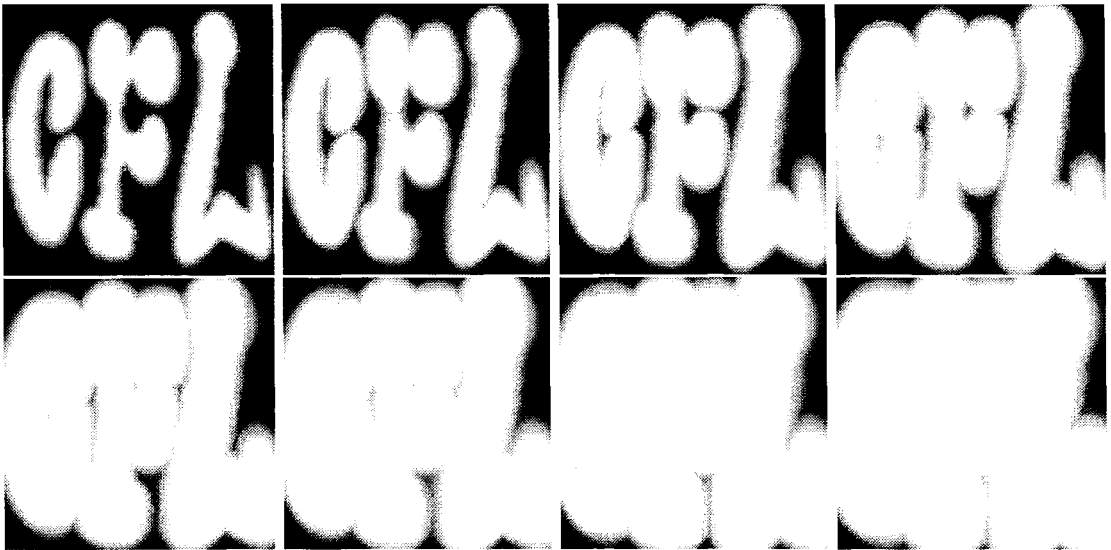


Figure 12. The images of the iterations (every two time steps)  $\Phi^2$  to  $\Phi^{16}$ , left to right, upper to bottom, for the scheme with non-violating (satisfying the CFL restriction) time step  $\Delta t = 0.7$ .

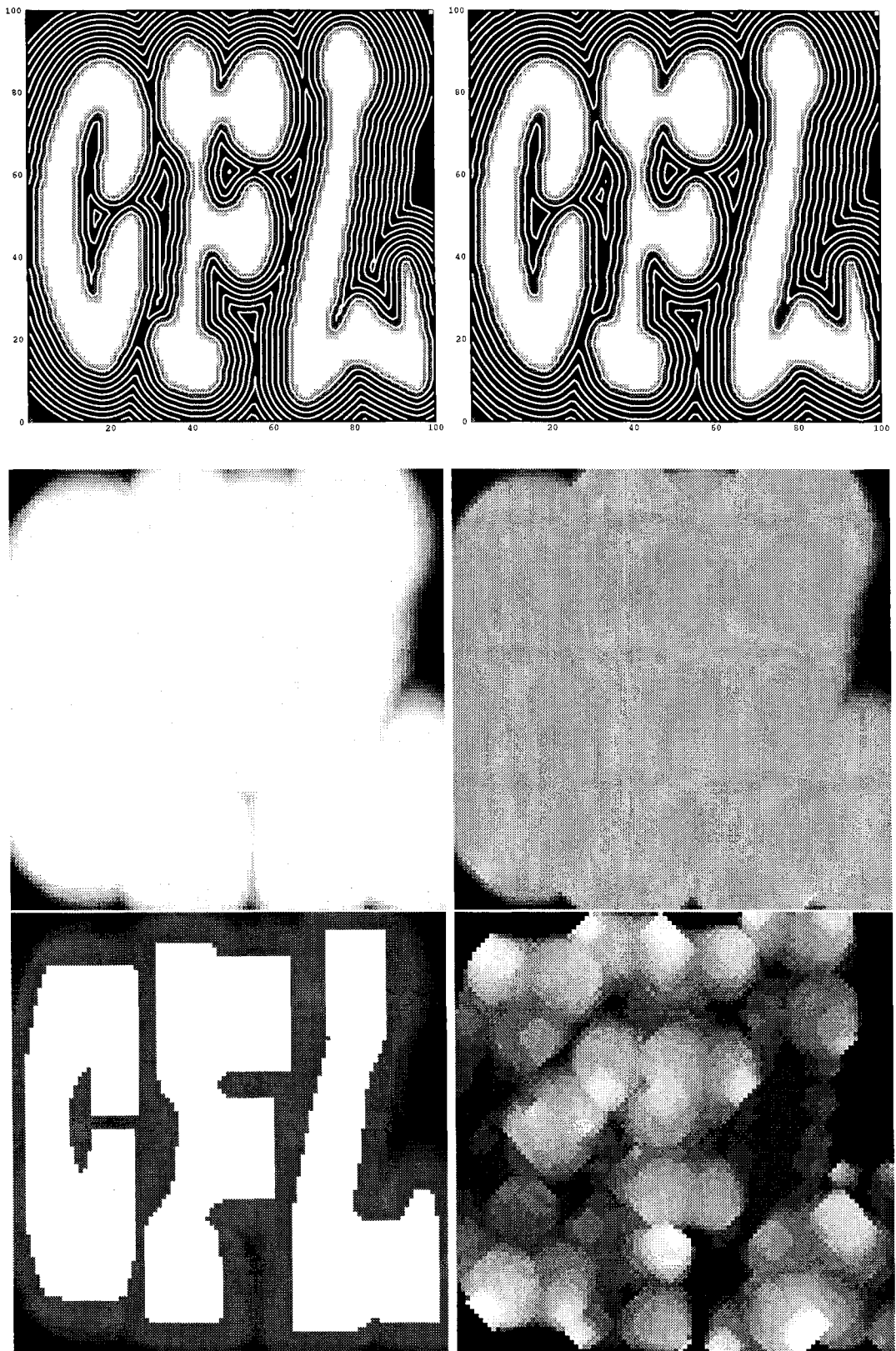


Figure 13. Left column:  $\Delta t = 0.7$ . Right column:  $\Delta t = 0.8$ , violating the CFL condition. Upper row: the offsets (zero level sets, of the propagating  $\Phi$  every two time steps) are shown as white contours on the original image. Middle row: the images of  $\Phi$  at  $t = 11.2$ , in which the heights  $\Phi_{ij}$  are presented as gray levels. Bottom row:  $\Phi$  images at  $t = 11.2$  after histogram equalization that stresses the instability effects caused by violating the CFL condition.

evolution step in order to strengthen the fact that violating the CFL restriction results in perturbations of the  $\Phi$  function. The bottom row in Fig. 13 shows the unstable result on the right compared with the stable one on the left. The zero level sets (every two time steps) are drawn as white contours on the original image (upper row). Since we have chosen only few iterations and selected a time step that is close to the CFL condition, the zero level sets are only slightly affected. More iterations or a larger time step will amplify the noise and distort the smoothness of the zero level sets.

## 11. Concluding Remarks

In this paper we reviewed the basic terminologies and methodologies in numerical analysis of conservation laws. Following Osher and Sethian, it was shown how planar curve evolution can be cast into the Eulerian formulation. This implicit formulation for curve evolution has the form of a Hamilton-Jacobi type of equation, for which there is a close relation to conservation laws. This relation was then explored and used to achieve efficient and stable numerical schemes.

The numerical schemes and limitations introduced in this paper were used in the cited papers in the design of finite difference approximations to the relevant PDEs. One important property of all the proposed numerical schemes is that when taking the discretization grid to a limit following the required limitations, the numerical schemes converge to the continuous case (the consistency property). This important property is lost for example when implementing graph search algorithms aimed at solving similar problems, since the metrics that the specific graphs induce inevitably lead to metrication errors.

## Acknowledgments

We thank the anonymous reviewers whose comments helped us to enhance the correctness and presentation of some of the topics we dealt with in this paper. We wish to thank our collaborators Doron Shaked, Yachin Pnueli, Guillermo Sapiro, Vicent Caselles and Laurent Cohen for letting us use figures from their works for illustrating the curve evolution based algorithms we referred to in this paper. RK's work is supported in part by the Applied Mathematics Subprogram of the Office of Energy Research under DE-AC03-76SFOO098, and ONR grant under N00014-96-1-0381.

## Notes

1.  $V$  may also depend on the global properties of the curve (e.g., (Sapiro and Tannenbaum, 1995)) as we will show, the relevant concept is for  $V$  to be *intrinsic*.
2.  $V_N$  is thus called an 'intrinsic' or 'geometric' quantity.
3. Observe that the numerical flux is a function  $g : \mathbb{R}^{p+q} \rightarrow \mathbb{R}$ , and thus maybe restricted as such to be Lipschitz.
4. See also (Harten et al., 1976).
5. Monotonicity does not necessarily hold for all upwind conservative schemes.

## References

- Adalsteinsson, D. and Sethian, J.A. 1995. A fast level set method for propagating interfaces. *J. of Comp. Phys.*, 118:269–277.
- Alvarez, L., Lions, P.L., and Morel, J.M. 1992. Image selective smoothing and edge detection by nonlinear diffusion. *SIAM J. Numer. Anal.*, 29:845–866.
- Alvarez, L., Guichard, F., Lions, P.L., and Morel, J.M. 1993. Axioms and fundamental equations of image processing. *Arch. Rational Mechanics*, 123.
- Blum, H. 1973. Biological shape and visual science ( part I). *J. Theor. Biol.*, 38:205–287.
- Brockett, R.W. and Maragos, P. 1992. Evolution equations for continuous-scale morphology. In *Proceedings IEEE International Conference on Acoustics, Speech, and Signal Processing*, San Francisco, California, pp. 1–4.
- Bruckstein, A.M. 1988. On shape from shading. *Comput. Vision Graphics Image Process.*, 44:139–154.
- Bruckstein, A.M. 1994. Analyzing and synthesizing images by evolving curves. In *Proceedings IEEE ICIP*, Austin, Texas, vol. 1, pp. 11–15.
- Caselles, V., Catta, F., Coll, T., and Dibos, F. 1993. A geometric model for active contours. *Numerische Mathematik*, 66:1–31.
- Caselles, V., Kimmel, R., and Sapiro, G. 1995a. Geodesic active contours. In *Proceedings ICCV'95*, Boston, Massachusetts, pp. 694–699.
- Caselles, V., Kimmel, R., and Sapiro, G. 1997. Geodesic active contours. *IJCV* 22(1):61–79.
- Chopp, D.L. 1993. Computing minimal surfaces via level set curvature flow. *J. of Computational Physics*, 106(1):77–91.
- Cohen, L.D. and Kimmel, R. 1997. Global minimum for active contour models: A minimal path approach. *IJCV* 24(1):57–78.
- Courant, R., Friedrichs, K.O., and Lewy, H. 1928. Über die partiellen differenzengleichungen der mathematischen Physik. *Math. Ann.*, 100:32–74.
- Courant, R., Friedrichs, K.O., and Lewy, H. 1967. On the partial difference equations of mathematical physics. *IBM Journal*, 11:215–235.
- Epstein, C.L. and Gage, M. 1987. The curve shortening flow. In *Wave Motion: Theory, Modeling, and Computation*. A. Chorin and A. Majda (Eds.), Springer-Verlag: New York.
- Feynman, R.P., Leighton, R.B., and Sands, M. 1964. *The Feynman Lectures on Physics*. Addison Wesley: Massachusetts.
- Gage, M. and Hamilton, R.S. 1986. The heat equation shrinking convex plane curves. *J. Diff. Geom.*, 23.

- Grayson, M. 1987. The heat equation shrinks embedded plane curves to round points. *J. Diff. Geom.*, 26.
- Harten, A., Hyman, J.M., and Lax, P.D. 1976. On finite-difference approximations and entropy conditions for shocks. *Comm. Pure Appl. Math.*, 29:297.
- Kimmel, R. 1992. Shape from shading via level sets. M.Sc. Thesis (in Hebrew), Technion—Israel Institute of Technology.
- Kimmel, R. 1995. Curve Evolution on Surfaces. D.Sc. Thesis, Technion—Israel Institute of Technology.
- Kimmel, R. and Bruckstein, A.M. 1993. Shape offsets via level sets. *CAD*, 25(5):154–162.
- Kimmel, R., Kiryati, N., and Bruckstein, A.M. 1994. Using multi-layer distance maps in finding shortest paths between moving obstacles. In *Proceedings of ICPR, International Conference of Pattern Recognition*, Jerusalem, Israel, pp. 367–372.
- Kimmel, R. and Bruckstein, A.M. 1995a. Global shape from shading. *CVIU*, 62(3):360–369.
- Kimmel, R. and Bruckstein, A.M. 1995b. Tracking level sets by level sets: A method for solving the shape from shading problem. *CVIU*, 62(2):47–58.
- Kimmel, R. and Sapiro, G. 1995. Shortening three dimensional curves via two dimensional flows. *International Journal: Computers & Mathematics with Applications*, 29(3):49–62.
- Kimmel, R., Shaked, D., Kiryati, N., and Bruckstein, A.M. 1995a. Skeletonization via distance maps and level sets. *CVIU*, 62(3):382–391.
- Kimmel, R., Siddiqi, K., Kimia, B.B., and Bruckstein, A.M. 1995b. Shape from shading: Level set propagation and viscosity solutions. *International Journal of Computer Vision*, 16:107–133.
- Kimmel, R., Amir, A., and Bruckstein, A.M. 1995c. Finding shortest paths on surfaces using level sets propagation. *IEEE Trans. on PAMI*, 17(6):635–640.
- Kimmel, R., Kiryati, N., and Bruckstein, A.M. 1996. Sub-pixel distance maps and weighted distance transforms. *Journal of Mathematical Imaging and Vision, Special Issue on Topology and Geometry in Computer Vision* (to appear).
- Kiryati, N. and Székely, G. 1993. Estimating shortest paths and minimal distances on digitized three dimensional surfaces. *Pattern Recognition*, 26(11):1623–1637.
- Kuznetsov, N.N. 1976. Accuracy of some approximate methods for computing the weak solutions of first-order quasi-linear equation. *USSR Comp. Math. and Math Phys.*, 16:105–119.
- Lax, P.D. 1973. *Hyperbolic Systems of Conservation Laws and the Mathematical Theory of Shock Waves*. Society for Industrial and Applied Mathematics: Philadelphia, Pennsylvania.
- LeVeque, R.J. 1992. *Numerical Methods for Conservation Laws*. Lectures in Mathematics. Birkhauser Verlag, Basel.
- Malladi, R., Sethian, J.A., and Vemuri, B.C. 1995. Shape modeling with front propagation: A level set approach. *IEEE Trans. on PAMI*, 17:158–175.
- Osher, S.J. and Sethian, J.A. 1988. Fronts propagating with curvature dependent speed: Algorithms based on Hamilton-Jacobi formulations. *J. of Comp. Phys.*, 79:12–49.
- Osher, S. and Shu, C.W. 1991. High-order essentially nonoscillatory schemes for Hamilton-Jacobi equations. *SIAM J. Numer. Anal.*, 28(4):907–922.
- Pnueli, Y. and Bruckstein, A.M. 1994. DigiDurer—a digital engraving system. *The Visual Computer*, 10:277–292.
- Pnueli, Y. and Bruckstein, A.M. 1996. Gridless halftoning. *Graphic Models and Image Processing*, 58(1):38–64.
- Sapiro, G. and Tannenbaum, A. 1993. Affine invariant scale-space. *International Journal of Computer Vision*, 11(1):25–44.
- Sapiro, G., Kimmel, R., Shaked, D., Kimia, B., and Bruckstein, A.M. 1993. Implementing continuous-scale morphology via curve evolution. *Pattern Recognition*, 26(9):1363–1372.
- Sapiro, G. and Tannenbaum, A. 1995. Area and length preserving geometric invariant scale-spaces. *IEEE Trans. on PAMI*, 17(1).
- Schroeder 1983. The eikonal equation. *The Mathematical Intelligencer*, 5(1):36–37.
- Sethian, J.A. 1985. Curvature and the evolution of fronts. *Commun. in Math. Phys.*, 101:487–499.
- Sethian, J.A. 1989. A review of recent numerical algorithms for hypersurfaces moving with curvature dependent speed. *J. of Diff. Geom.*, 33:131–161.
- Shaked, D. and Bruckstein, A.M. 1995. The curve axis. *CGIU* (to appear).
- Smoller, J. 1983. *Shock Waves and Reaction-Diffusion Equations*. Springer-Verlag: New York.
- Sod, G.A. *Numerical Methods in Fluid Dynamics*. Cambridge Univ. Press.
- Weickert, J., Anisotropic diffusion in image processing. Ph.D. Thesis. Kaiserslautern Univ. Germany, Nov. 1995.